environments

MDPI

Article

Valorization of Pinecones as Biosorbents for Environmental Remediation of Zn-Contaminated Wastewaters

Morgana Macena [1,2,*], Luísa Cruz-Lopes [2], Lucas Grosche [3], Bruno Esteves [2], Isabel Santos-Vieira [4] and Helena Pereira [1,*]

[1] CEF-Forest Research Centre, Associate Laboratory TERRA, School of Agriculture, University of Lisbon, 1349-017 Lisboa, Portugal
[2] CERNAS-IPV Research Centre, Polytechnic University of Viseu, Campus Politécnico, Repeses, 3504-510 Viseu, Portugal; lvalente@estgv.ipv.pt (L.C.-L.); bruno@estgv.ipv.pt (B.E.)
[3] 4iTec Lusitânia S.A., Lugar do Pombal, Zona Industrial do Salgueiro, 3530-259 Mangualde, Portugal; lucas.grosche@4iteclusitania.pt
[4] CICECO—Aveiro Institute of Materials, Department of Chemistry, University of Aveiro, 3810-193 Aveiro, Portugal; ivieira@ua.pt
* Correspondence: morgana@estgv.ipv.pt (M.M.); hpereira@isa.ulisboa.pt (H.P.)

Abstract

Empty pinecones are a largely available byproduct of *Pinus pinea* L. nut production, mostly concentrated in the Mediterranean area; e.g., in Portugal, around 70,000 tons of pinecones are produced annually. One valorization line for residual biomass is its use as biosorbents for the removal of contaminants in effluents and water courses which are an increasing environmental problem. This study explores the biosorbent potential of pinecones to remove zinc ions from aqueous solutions. We analyzed the morphology and chemical composition of pinecones (9.4% extractives, 37.0% lignin, 68.6% holocellulose, 1.4% ash). The effect of pH and adsorbent dose on the adsorption process was studied, as were the sorption kinetics and isotherms. The pinecones showed good potential to remove Zn ions, with 96% removal at pH 7 and a maximum adsorption capacity of 7.92 mg g^{-1}. The process followed the Freundlich isotherm model, indicating a heterogeneous surface and multilayer adsorption, and the pseudo-second-order kinetic model, suggesting chemisorption as the dominant mechanism. The use of pinecones as bio-adsorbent is therefore a green and low-cost alternative for environmental remediation and biomass waste management.

Keywords: pinecones; wastewater treatment; biosorption; zinc removal; byproducts valorization

Academic Editors: Athanasia Tolkou and George Z. Kyzas

Received: 20 June 2025
Revised: 14 August 2025
Accepted: 15 August 2025
Published: 17 August 2025

Citation: Macena, M.; Cruz-Lopes, L.; Grosche, L.; Esteves, B.; Santos-Vieira, I.; Pereira, H. Valorization of Pinecones as Biosorbents for Environmental Remediation of Zn-Contaminated Wastewaters. *Environments* **2025**, *12*, 284. https://doi.org/10.3390/environments12080284

1. Introduction

Pine species constitute one of the most commercially valuable groups of forest trees, extensively utilized in industrial wood processing and as sources of non-timber forest products [1]. Approximately 130 species of pines (*Pinus* spp.) are recognized, originating primarily in the Northern Hemisphere, with some species also native to Southern Africa and Australia [2]. Today, they are cultivated across diverse regions worldwide. The stone pine (*Pinus pinea* L.) is among the most prominent species, widely cultivated throughout the Mediterranean basin, particularly in Spain, Portugal, Italy, Greece, Albania, and Turkey [3].

The primary economic use of the stone pine is the production of edible pine nuts (pinions), which possess high commercial and nutritional value [4], ranking among the most significant non-timber forest products in Mediterranean countries [5]. The industrial processing of pinions after the field collection of the pinecones includes the cone opening,

the separation of woody parts from the shelled nuts, and the subsequent shell crushing and nut peeling [5]. The pinecones are a byproduct of this production, concentrated in large quantities at the processing mills, estimated at 200–600 kg/ha, and a total of 70,000 tons of stone pinecones are produced every year in Portugal [6,7].

Biomass residues generated from agro-industrial and agroforestry activities, often burned or discarded in the field, are increasingly targeted for valorization within integrated waste management strategies aimed at generating economic value and mitigating environmental impacts [8]. One valorization route for lignocellulosic wastes lies in their capacity to bind metal ions, which is attributed to their porous structures and diverse surface functional groups, such as carboxyl and hydroxyl [9,10].

The removal of heavy metals from wastewater is a matter of great interest given their toxicity and lack of biodegradability being a threat to both ecosystems and human health [11]. Common pollutants in industrial effluents include cadmium (Cd), chromium (Cr), copper (Cu), lead (Pb), nickel (Ni), and zinc (Zn) [8]. Adsorption is a particularly important method for water treatment [2]. Among the various sorbents that are commercially used or under investigation, biosorbents consisting of dead and live biomass are very much in the limelight since their use in biosorption is a low-cost and effective treatment to eliminate heavy metals from industrial wastewater via multiple binding mechanisms [11,12].

Pine-derived wastes, including wood, sawdust, bark, needles, and cones, are abundant globally and have been investigated as cost-effective biosorbents for metal ion removal [13]. The removal of Cu(II) and Cd(II) by biosorption with pinecones was analyzed and showed promising results [14]. Milled pinecones (*Pinus halepensis* and *Pinus pinea*) were applied to remove Pb(II), Cd(II), Cu(II), and Cr(VI) from aqueous solution achieving good removal efficiency [11]. Another study tested carboxylate-modified pinecones in the removal of Pb ions and obtained high adsorption levels [10]. The bark powder of *Pinus brutia* and a mixture of *Pinus pinaster*, *Pinus radiata*, *Pinus pinea,* and *Pinus sylvestris* were tested as biosorbents to remove Pb [15], and Fe, Cu, Zn, Cd, Ni, Pb, and Sn ions showed good capabilities for the adsorption of metal ions [14,16]. Pine sawdust (*Pinus sylvestris*) was applied to adsorb Cd(II) and Pb(II) ions, achieving removal rates of 96% for Cd and 98% for Pb [17]. However, few studies have specifically addressed Zn(II) biosorption or correlated the chemical properties of the biomass with its adsorption potential.

Zn(II) removal from aqueous solutions, under both mono- and multi-metal conditions, has been explored using biomasses such as clarified sludge, rice husk ash, neem bark, activated alumina [18], *P. pinaster* bark [19], crab shell [20], *Lemna gibba* [21], *Ziziphus joazeiro* barks [22], and *Sargassum ilicifolium* [23]. Overall, the biosorption of zinc ions was effective, although pH, contact time, biosorbent dosage, initial metal concentration, and kinetic and isotherm models varied across the adsorbents. Spectroscopic and microscopic analyses confirmed the involvement of functional groups (e.g., carboxyl) in the metal binding mechanism.

In the present study, we explored the biosorbent potential of stone pinecones (SPCs) and their applicability to remove zinc ions from aqueous solutions. The rationale for this approach is rooted in the large-scale availability of pinecones at pine nut processing mills, their favorable handling properties, and suitable physicochemical characteristics. Additionally, pinecones are a low-value byproduct, often discarded or used as bulk biomass for energy.

Chemical composition was determined using wet chemical analysis and Fourier-transform infrared spectroscopy (ATR-FTIR). Physical properties were studied by scanning electron microscopy (SEM), thermogravimetric analysis (TGA), and powder X-ray diffraction (XRD) measurements. Batch adsorption experiments were conducted with granulated

pinecones, assessing the effects of pH, adsorbent dosage, and particle size, alongside kinetic and isotherm modeling.

2. Materials and Methods

2.1. Sample Preparation

The stone pinecones (SPCs) used in this study were collected as residues from pine nut processing mills, supplied by local producers in the Viseu region, Portugal. The cones were milled using a Retsch SMI mill and sieved (Retsch AS200) to obtain three particle size fractions, 40–60 mesh (0.420–0.250 mm), 60–80 mesh (0.250–0.177 mm), and <80 mesh (<0.177 mm), which were subsequently used in the experiments. Samples were oven-dried at 105 °C for at least 2 h to ensure complete moisture removal before use.

To evaluate the intrinsic adsorption capacity of the pinecones, no chemical or thermal pre-treatment was applied, thus preserving their natural composition. This minimal processing approach, with low energy requirements, aligns with the broader goal of assessing SPCs as a sustainable, low-cost biosorbent suitable for large-scale water treatment applications.

Stock solutions of Zn(II) were prepared from $Zn(NO_3)_2$ in distilled water at target concentrations, 10, 20, 30, 40, and 50 mg L^{-1}, for batch adsorption experiments.

2.2. Chemical Characterization of Pinecones

The chemical characterization involved the quantification of extractives, holocellulose, α-cellulose, lignin, ash, and inorganic cationic contents. All analyses were conducted with the 40–60 mesh fraction, in triplicate, to ensure reproducibility and accuracy.

Sequential extractions were carried out using dichloromethane, ethanol, and water in accordance with the TAPPI T 204 standard [24]. Cellulose content was determined following the Kürschner and Höffner method. Holocellulose was determined via the acid-chlorite method using extractive-free material. The determination of α-cellulose was performed following the TAPPI T 203 procedure [25]. The content of hemicelluloses was estimated as the difference between the contents of holocellulose and α-cellulose. Lignin content was analyzed according to the TAPPI T 222 standard [26], including Klason lignin (insoluble fraction) and the acid-soluble lignin measured spectrophotometrically at 205 nm.

Ash content was determined by calcination in a muffle furnace at 525 °C until white ash was obtained. For cation quantification, ashes were digested in 65% nitric acid, and the concentrations of Ca, Mg, K, Na, and Zn were measured using a flame atomic absorption spectrophotometer (AAS, Perkin Elmer AAnalyst 300, Shelton, CT, USA).

Attenuated total reflectance Fourier-transform infrared (ATR-FTIR) spectra were obtained using a PerkinElmer Spectrum Two spectrometer. Spectra were acquired over the range of 4000–500 cm^{-1} at a resolution of 4.0 cm^{-1} with a scanning rate of 10 scans per minute. Prior to analysis, samples were oven-dried at 100 °C. For spectral acquisition, powdered samples (<80 mesh) were pressed directly against the ATR crystal.

The point of zero charge (pHpzc) was determined by adding 0.10 ± 0.05 g of <80 mesh sample to 25 mL of distilled water adjusted to pH 2–12 (NaOH or HCl, 0.1 M), followed by 24 h agitation at room temperature. Initial and final pH values were recorded (HACH HQ 30d pH meter), and pHpzc was identified as the pH range where the buffering effect occurred.

2.3. Physical Properties and Pinecone Surface Characteristics

All the physical analyses and characterization were made with the powder fraction (<80 mesh).

High-resolution scanning electron microscopy (SEM) was performed on a Hitachi SU-70 (Monocomp) microscope (Hitachi High-Tech Corporation, Tokyo, Japan), operated at an accelerating voltage of 15 kV. Samples were mounted on aluminum stubs and coated with a conductive carbon layer using an Emitech K950X carbon evaporator.

Powder X-ray diffraction (XRD) measurements were carried out on an Empyrean PANalytical diffractometer (Malvern Panalytical B.V., Almelo, The Netherlands) equipped with a PIXcel 1D detector and operated in Bragg–Brentano para-focusing geometry. The instrument utilized Cu Kα radiation (λ_1 = 1.540598 Å, λ_2 = 1.544426 Å) with operating conditions of 45 kV and 40 mA. Diffraction data were collected in continuous scan mode over the 2θ range of 3.5° to 50°, with a step size of 0.01°.

Thermogravimetric analysis (TGA) was conducted using a Mettler V3 thermobalance coupled with a TC10A processor (Mettler-Toledo AG, Greifensee, Switzerland), with heating from ambient temperature to 800 °C at 5 °C min^{-1}.

2.4. Adsorption Studies

The effects of particle size (40–60 mesh, 60–80 mesh, and <80 mesh), adsorbent dosage (based on particle size efficiency), and pH (range 3–9) on Zn(II) removal were evaluated by carrying out batch adsorption experiments. All tests were conducted in triplicate, using an initial Zn(II) concentration of 20 mg L^{-1}, 240 min contact time, and room temperature.

To study the isotherms, tests were performed with increasing concentrations of Zn ions, from 10 to 50 mg L^{-1}, and the Langmuir (Equation (1)) and Freundlich (Equation (2)) models were analyzed. In the kinetic tests, time variation was between 1 and 30 min, with a Zn concentration of 20 mg L^{-1}, and the pseudo-first (PFO) and pseudo-second-order (PSO) (Equations (3) and (4), respectively), Elovich (Equation (5)) and Intraparticle Diffusion (ID) (Equation (6)) models were analyzed. The quantification of the remaining metals in solution was performed by AAS. The adsorption rate (%) was given by the difference between the initial and final concentration of the metal ion measured in the solution in percentage of the initial concentration (Equation (7)).

$$\frac{1}{q_e} = \frac{1}{q_{max}} + \left(\frac{1}{K_L q_{max}}\right) \times \frac{1}{C_e} \quad (1)$$

$$logq_e = logK_F + \frac{1}{n} logC_e \quad (2)$$

$$ln(q_e - q_t) = lnq_e - k_1 t \quad (3)$$

$$\frac{t}{q_t} = \frac{1}{k_2 q_e^2} + \frac{t}{q_e} \quad (4)$$

$$q = \left(\frac{1}{b}\right) ln(ab) + \left(\frac{1}{b}\right) lnt \quad (5)$$

$$q_t = k_{int} t^{\frac{1}{2}} + C \quad (6)$$

$$\%adsorption = \left(\frac{Ci - Cf}{Ci}\right) \times 100 \quad (7)$$

where *qe* (mg g^{-1}) represents the quantity of ions adsorbed in each g of adsorbent material, *qmax* corresponds to the saturation capacity of the adsorbent material, *Ce* (mg L^{-1}) is the equilibrium concentration, and *KL* is the Langmuir constant. The *n* is the Freundlich parameter, which indicates the magnitude of the surface heterogeneity. The *qt* (mg g^{-1}) represents the adsorbed quantity at time t; k_1 (min), k_2 (g mg^{-1}.min), and *kint* (mg g^{-1} min$^{1/2}$) are the corresponding adsorption rate constants; *a* (mg g^{-1}.min) is the initial sorption rate constant; and *b* (g mg^{-1}) is related to surface coverage. *Ci* is the initial

concentration of the metal in the solution (mg L^{-1}), and *Cf* is the concentration of the metal remaining in the solution (mg L^{-1}) after the adsorption process, measured by AAS.

3. Results

3.1. Chemical Composition, Ash, and Cationic Content

The results for the chemical composition and point of zero charge (pHpzc) are presented in Table 1. Theinorganic cation contents of SPCs are presented in Table 2.

Table 1. Chemical characterization of *Pinus pinea* cones (SPCs), expressed as a percentage of the initial dry mass (%).

Parameter	Value
Total extractives (%)	9.4 ± 0.39
Dichloromethane extractives (%)	3.6 ± 0.25
Ethanol extractives (%)	4.8 ± 0.86
Water extractives (%)	1.0 ± 0.67
Total lignin (%)	37.0 ± 0.44
Klason lignin (%)	36.9 ± 0.42
Soluble lignin (%)	0.1 ± 0.03
Holocellulose (%)	68.6 ± 0.38
α-cellulose (%)	49.0 ± 0.81
Hemicelluloses (%)	19.6 ± 1.07
Ashes (%)	1.4 ± 0.2
pHpzc	5.2

Table 2. Cationic contents in the ashes obtained from *Pinus pinea* cones (SPCs), presented in milligrams per gram of initial dry mass (mg g^{-1}).

	Element				
	Ca	**Na**	**Mg**	**Zn**	**K**
Content (mg g^{-1})	0.15	0.20	0.46	0.001	1.72

The pinecones exhibited a relatively high content of total extractives (9.4%), of which 38% consisted of lipophilic compounds extracted with dichloromethane. Lignin content was high (37.0%), while the α-cellulose and hemicellulose contents were also significant (49.0% and 19.6%, respectively). Ash content was low (1.4%), with potassium (1.72 mg g^{-1}) being the most abundant element detected.

3.2. Fourier-Transform Infrared Spectroscopy (ATR-FTIR)

The ATR-FTIR spectrum obtained for the SPC samples is shown in Figure 1, as the average of three independent measurements.

The spectrum is characterized by a broad band at approximately 3336 cm^{-1} recognized as O-H stretching of hydroxyl groups, a band between 2826 and 2980 cm^{-1}, characteristic of the presence of CH_2 stretch, a peak at 1724 cm^{-1} from C=O groups, and a sharp peak at 1505 cm^{-1} and a broad peak around 1606 cm^{-1} which are characteristic of aromatic skeleton vibration of lignin. The spectrum is dominated by a large and broad peak at around 1027 cm^{-1} characteristic of C-O, CC, and C-CO stretch in cellulose, hemicelluloses, and lignin.

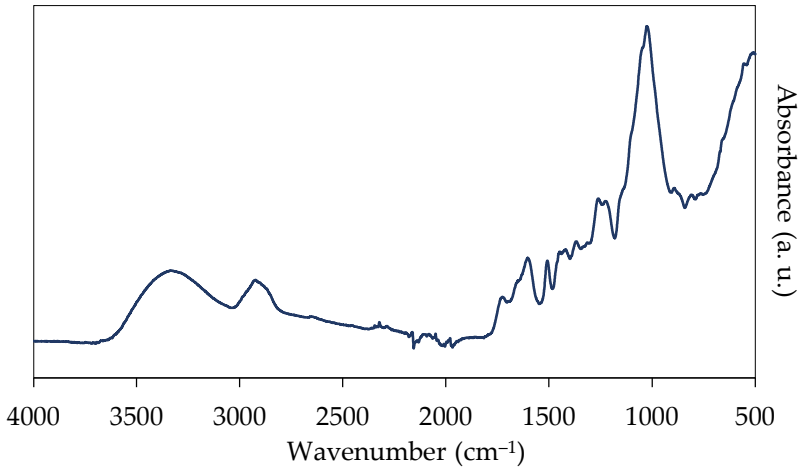

Figure 1. ATR-FTIR spectra of *Pinus pinea* cone powder (<80 mesh) samples.

3.3. Pinecone Surface Characteristics

3.3.1. Scanning Electron Microscopy (SEM)

SEM micrographs (Figure 2) revealed SPC particles with a fragmented cellular structure, exposing both surface and cross-sectional views of cell walls. The material appeared heterogeneous, irregular, and porous, with multiple cracks and voids. Due to the small particle size (<177 µm) used, intact cells (e.g., tracheids) were not observed.

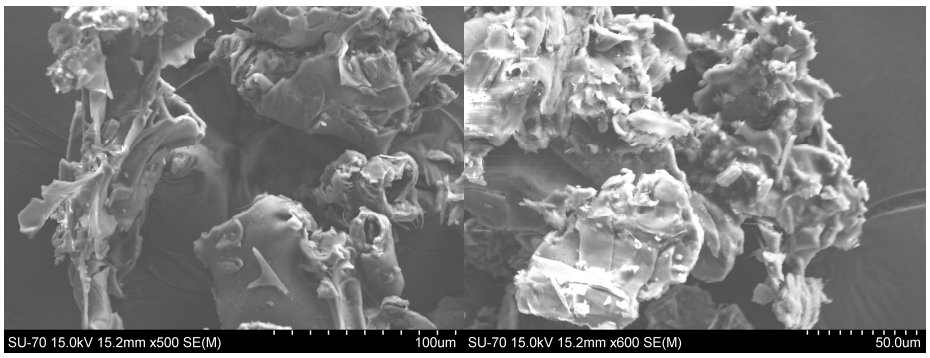

(**a**) (**b**)

Figure 2. SEM images of the surface of powder samples (>180 µm) of *Pinus pinea* cones (SPCs), at magnifications of 500× (**a**) and 600× (**b**).

3.3.2. Powder X-Ray Diffraction (XRD)

The diffractogram obtained for the pinecone samples is presented in Figure 3.

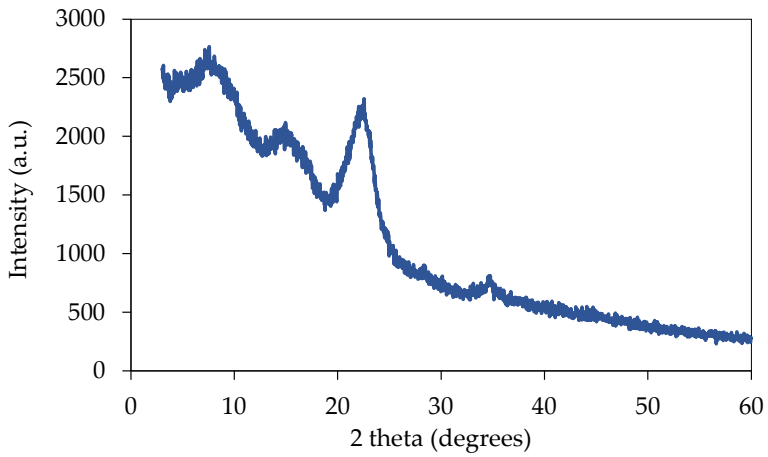

Figure 3. Powder X-ray diffractogram of the *Pinus pinea* cone (SPC) powder sample (>80 mesh).

Characteristic peaks for cellulose identified (2 theta) at 15.7°, 21.3°, and 34.4° [27] were present in the SPC powder sample. Another peak at approximately 10° was also observed.

3.3.3. Thermogravimetric Analysis (TGA)

The thermal analysis curves, thermogravimetric (TG) and derivative thermogravimetric (DTG) of SPCs are presented in Figure 4.

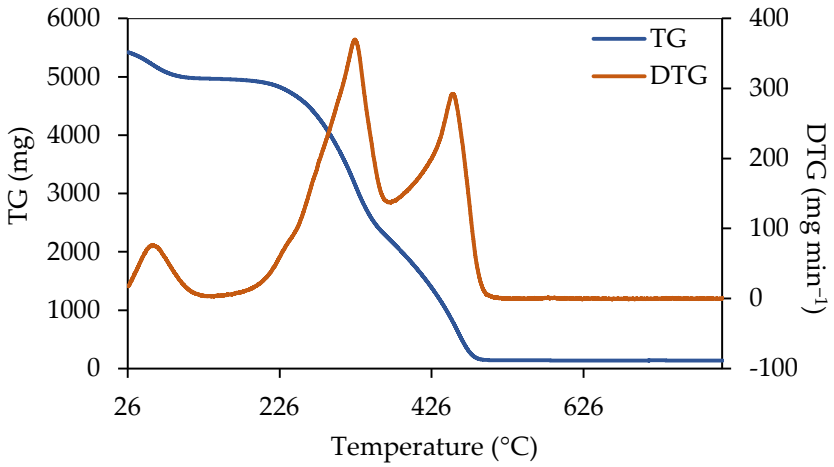

Figure 4. Thermal analysis curves (TG and DTG) of *Pinus pinea* cones (SPCs).

The thermal analysis of SPCs reveals important insights into their decomposition behavior. The TG curve shows a gradual decrease in mass as the temperature increases, and different phases were observed: an initial small mass decrease until about 100 °C, followed by a short plateau until about 230 °C, when mass loss started, with a significant drop occurring until approximately 480 °C, with a small inflection at 365 °C, corresponding to the major degradation phase. Subsequently, the mass remains constant, and the high residual mass observed at around 600 °C suggests a substantial content of fixed carbon or ash.

The DTG curve presents three distinct degradation peaks at approximately 80, 330, and 450 °C. The first peak (~80 °C) is associated with the evaporation of moisture or volatile compounds. The second, more intense peak (~330 °C) corresponds to the degradation of hemicelluloses and the onset of cellulose and lignin decomposition. The third peak (~450 °C) is attributed to the thermal breakdown of cellulose and lignin, and resistant components such as resins and phenolic compounds.

3.4. Adsorption Tests

3.4.1. Effect of Particle Size

The experimental results of the SPC particle size influence on the adsorption process of zinc ions are presented in Table 3.

Table 3. Influence of particle size of *Pinus pinea* cones (SPCs) in the sorption of Zn ions measured as the removal rate in % of the initial concentration (20 mg L^{-1}).

Granulometry (Mesh)	Particle Size (mm)	Removal Rate (%)
40–60	0.420–0.250	95.3
60–80	0.250–0.177	96.1
<80	<0.177	96.4

No significant difference was observed between the particle sizes tested, with the sorption rates for all particle sizes around 96%. Therefore, it was decided to use the smallest

particle size (<0.177 mm) in the current experiments in order to have the greatest surface area of contact between the adsorbate and adsorbent.

3.4.2. Effect of Adsorbent Dosage

The amount of adsorbent used plays a significant role in the adsorption process, since the number of active sites available to bind the zinc ions is directly related to the mass of adsorbent. The effect of adsorbent dose was tested by increasing the dosage of the SPC biosorbent from 1 to 8 g L^{-1}, with an initial Zn concentration of 20 mg L^{-1}. The results obtained are shown in Figure 5.

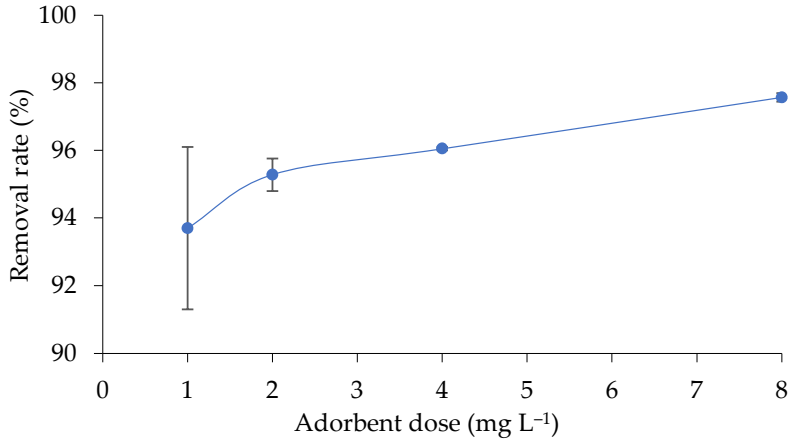

Figure 5. Influence of the adsorbent dose of Pinus pinea cones (SPCs) as powder samples (> 80 mesh) in the sorption rate of Zn ions measured as the removal rate in % of the initial concentration (20 mg L^{-1}).

Adsorption rates higher than 90% were obtained for all the experimentally tested dosages. The adsorption increased when increasing the adsorbent dose from 1 to 2 g L^{-1}, but between 2 and 8 g L^{-1}, only a slight difference was observed. Since good results were achieved with 4 g L^{-1}, this dosage was used for the following experimental studies to avoid particle aggregation and to reduce the cost of the process.

3.4.3. Effect of pH

The pH can modify the way that metal ions are available in the solution, limiting the sorption rate. The influence of pH in the solution was tested with a pH range from 3 to 9, as shown in Figure 6.

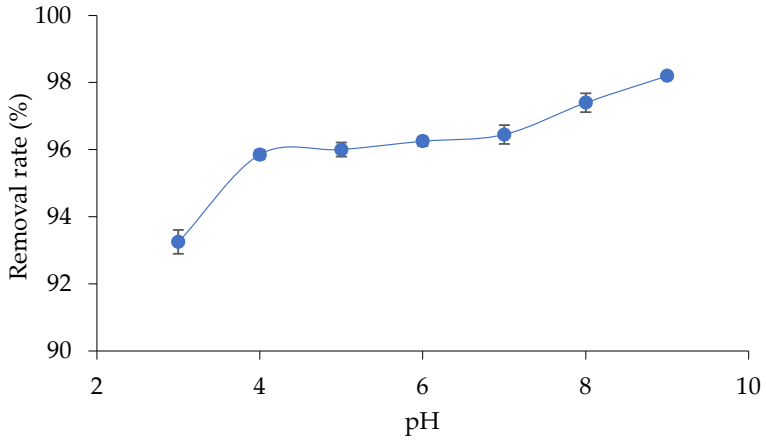

Figure 6. Influence of the pH on the adsorption rate of Zn ions by *Pinus pinea* cones (SPCs) as powder samples (>80 mesh, 4 g L^{-1}) measured as the removal rate in % of the initial concentration (20 mg L^{-1}).

Good results were achieved within all the pH ranges tested, with adsorption rates between 93 and 98%, although an increase in the sorption rate was noted with the increase in the pH. However, at pH 8–9, precipitation of zinc in the form of $Zn(OH)_2$ can occur, which may have influenced the results. Therefore, a pH of 7 was selected as ideal for binding Zn ions onto the SPC biosorbent.

3.4.4. Adsorption Isotherms

The isotherms describe the way adsorption occurs on the surface of the adsorbent material. The effect of the initial concentration of Zn ions on the adsorption rate is presented in Figure 7.

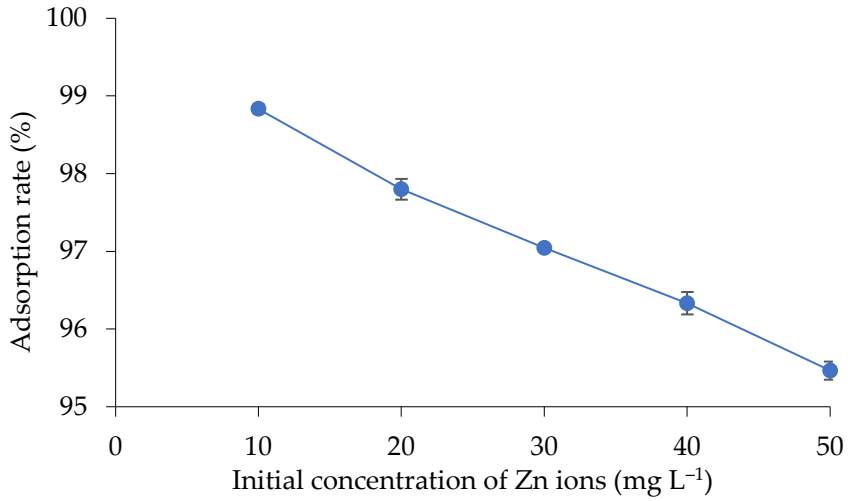

Figure 7. Effect of the initial concentration of zinc ions (10–50 mg L^{-1}) on the adsorption rate on *Pinus pinea* cones (SPCs) as powder samples (> 80 mesh, 4 g L^{-1}) measured as the removal rate in % of the initial concentration.

The isotherm experimental results were plotted according to the Langmuir and Freundlich models, as shown in Figure 8. The parameters obtained for the models are presented in Table 4.

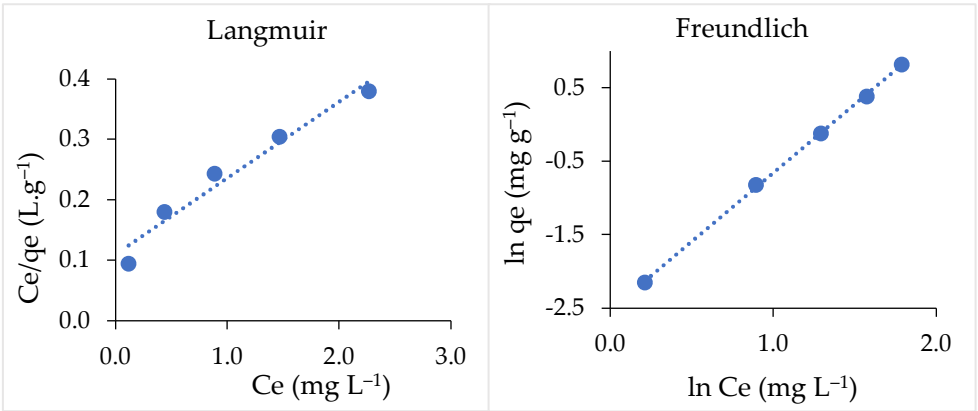

Figure 8. Plotting of the experimental results of the *Pinus pinea* cones (SPCs) adsorption isotherm of zinc ions according to the Langmuir and Freundlich models.

According to the correlation obtained, the adsorption of zinc onto SPCs follows the Freundlich model (R^2 = 0.999), characterized by a multilayer deposition with heterogeneous forces of adsorption.

Table 4. Parameters found for Langmuir and Freundlich isotherm models for the adsorption of zinc ions by *Pinus pinea* cones (SPCs).

Langmuir			Freundlich		
R^2	*qmax* (mg g^{-1})	*KL* (L mg^{-1})	R^2	*n*	*KF* (mg g^{-1})
0.96	7.92	1.15	0.99	0.54	0.08

3.4.5. Adsorption Kinetics

The kinetics elucidates the speediness of the reaction and allows insight into the binding mechanisms between adsorbate and adsorbent. The plotting of contact time and initial concentration is given in Figure 9.

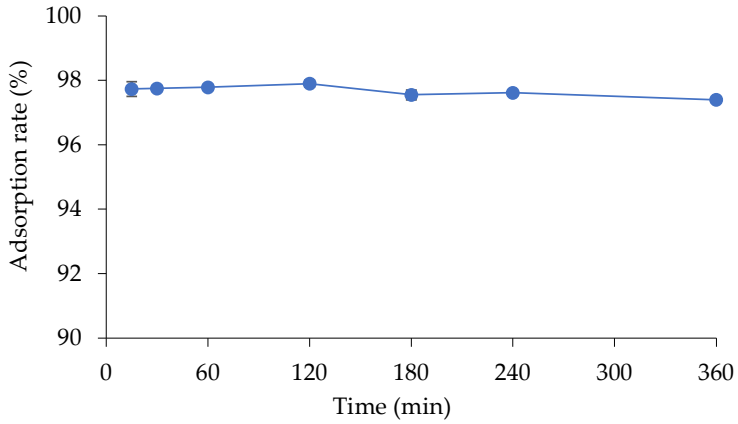

Figure 9. Adsorption rate of Zn ions over contact time with pinecone adsorbent.

Four kinetic models were tested, PFO, PSO, Elovich, and ID, as shown in Figure 10, and the results are given in Table 5.

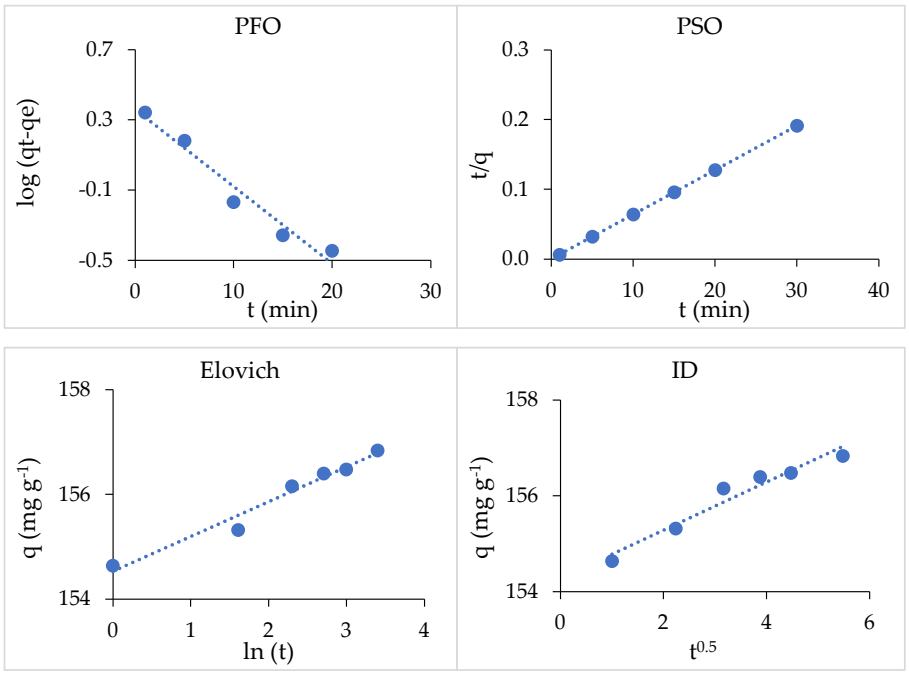

Figure 10. Plotting of the experimental results of *Pinus pinea* cones (SPCs) adsorption kinetics according to the PFO, PSO, Elovich, and ID models.

Table 5. Mathematical parameters of the pseudo-first- and pseudo-second-order, Elovich, and Intraparticle Diffusion kinetic models found for the adsorption of Zn by *Pinus pinea* cones (SPCs).

PFO				PSO					Elovich			ID		
K1 (L min^{-1})	*qe* (mg g^{-1})	*qe* exp (mg g^{-1})	R^2	*K2* (g mg^{-1}.min)	*h* (mg g^{-1}.min)	*qe* (mg g^{-1})	*qe* exp (mg g^{-1})	R^2	*a*	*b*	R^2	*C*	*kdif*	R^2
0.04	1.43	156.84	0.96	0.006	1.00	156.25	156.84	1	0.66	154.53	0.97	154.28	0.50	0.95

According to the correlation results, the adsorption of Zn ions onto pinecones occurs mostly by chemisorption, following the PSO model, with experimental and modeling results totally fitted ($R^2 = 1$). However, the other models tested also presented good correlations, which means that more than one mechanism may take place along the sorption process. The equilibrium or saturation point of the adsorbent was observed at around 30 min.

4. Discussion

4.1. Chemical Characterization of Pinecones (SPCs)

The chemical composition of SPCs (Table 1) is consistent with the limited literature available for *Pinus pinea* cones. For instance, cones collected from various regions of Turkey contained 0.8–1.5% ash, 5.2–7.5% cyclohexane–ethanol extractives, 34.5–38.8% lignin, 52.3–57.1% holocellulose, and 35.8–39.0% α-cellulose [28]. Compositional variability has been reported for pinecones from other Pinus species; they generally exhibit elevated extractives and lignin content, as reported for *P. pinaster* [29] and *P. nigra* [30].

The main chemical constituents of SPCs are cellulose, hemicelluloses, and lignin, which all contain functional groups of interest to the chemisorption of metal ions. Cellulose is a linear glucose polymer containing hydroxyl (–OH) groups, contributing to hydrogen bonding, while hemicelluloses are amorphous polymers with more accessible OH groups and include other more functional groups, e.g., ester and acid, increasing the number of active sites. Lignin contains methoxyl, phenolic, and carboxyl groups that interact with contaminants.

The point of zero charge (pHpzc) of SPCs was 5.2 (Table 1), similar to the value of 5.6 found for Pinus spp. cones [1] although lower than that found for pinecones from Tunisia (6.2) [9].

BET analysis yielded negligible measurable surface area, suggesting that SPCs predominantly contain macropores, which contribute minimally to total surface area compared with meso- and micropores. Consequently, metal ion adsorption by SPCs is likely governed primarily by surface functional group chemistry (e.g., –OH and –COOH) rather than by physical surface area, with chemical interactions such as chelation and ion exchange predominating.

The ATR-FTIR spectra (Figure 1) displays characteristic bands of extractives, lignin, cellulose, and hemicelluloses, in agreement with previous reports for pinecones. A similar spectral pattern of functional groups was observed: O–H stretching vibrations of the hydrogen-bonded hydroxyl group, C–H stretching vibration of the aliphatic group, C=O stretching vibrations of the carboxyl groups, and C-O stretching vibration of the primary alcohol groups [9,11,31]. Additional features were observed, such as carboxylic/aromatic hydroxyl (–OH) stretching of the phenol group at 1386 cm^{-1} and 1268 cm^{-1} [11], C=C aromatic ring stretching vibration at 1580 cm^{-1}, phosphoric compounds around 1200 cm^{-1}, stretching vibrations of hydrogen-bonded P=O at 1173 cm^{-1}, and acid phosphate esters at 1072 cm^{-1} [31].

In summary, the chemical characteristics of SPCs highlight their potential as effective biosorbents due to the abundance of functional groups such as hydroxyl, carboxyl, methoxyl, and phenolic groups. These groups, primarily located within cellulose, hemicel-

luloses, and lignin, facilitate diverse interactions with metal ions, including coordination, electrostatic attraction, ion exchange, and complexation. The observed chemical features, supported by ATR-FTIR analysis and pHpzc data, align with prior findings for *Pinus* species and underscore the suitability of SPCs for metal ion adsorption.

4.2. Surface Morphology and Structural Analysis

SEM micrographs (Figure 2) reveal that SPC particles exhibit a fragmented and irregular cellular structure. The surface morphology is heterogeneous and porous, with multiple fissures and voids distributed across the matrix. This architecture increases the accessibility of internal functional groups, potentially enhancing sorption kinetics. Likewise, in pinecones from Tunisia, the SEM images before adsorption revealed an irregular and uneven surface [9]. The same pattern was described for *Pinus halepensis* cones [32].

Crystallinity plays a critical role in adsorption processes, particularly in polymeric and particulate adsorbent materials, due to its influence on the solid structural organization. Materials with higher degrees of crystallinity can exhibit a reduced surface area, leading to the lower availability of active sites. Conversely, a crystalline structure may also impact the diffusional pathways of adsorbates, thereby affecting both the adsorption kinetics and the overall uptake capacity. XRD analysis of pinecones identified characteristic peaks for cellulose (2 theta) at 15.7°, 21.3°, and 34.4° [27]. These peaks were also identified in SPCs in this work (Figure 3), at 2θ = 16°, 22°, and 34°, which indicates that the structure is mainly organized with crystalline cellulose [9]. XRD analysis of milled pinecone shells from Tunisia showed a broad peak from 11° to 34° (2θ), which characterizes the amorphous phase, as observed in biosorbents constituted by lignin, hemicelluloses, and amorphous cellulose [9]. This broad peak was not identified in this work.

The thermal decomposition profile of SPCs (Figure 4) is characterized by an initial mass loss of up to ~100 °C, attributed to moisture and volatile organic compounds, followed by a minor plateau until ~230 °C. The major degradation stage occurs between ~230 °C and 480 °C, with an inflection near 365 °C, indicative of overlapping hemicellulose, cellulose, and lignin decomposition. A third degradation event near 450 °C is associated with thermally stable fractions such as lignin-derived aromatics, resins, and phenolic compounds. The substantial residual mass at 600 °C reflects a high fixed carbon and mineral ash content, consistent with the elemental analysis. This behavior is related to the high content of lignin and extractives, such as resins and phenolic compounds, typically found in conifers [33].

A study with pinecones from Spain reported that the loss in weight between 175 and 200 °C corresponds to equilibrium moisture content, while from 200 to 300 °C, less stable constituents are decomposed, like hemicelluloses, and between 300 and 400 °C, the degradation of cellulose occurs [34]. Similar results were reported in the thermal analysis of pinecones from China, for which the DTG curve demonstrated two weight loss peaks at approximately 300 and 450 °C, with the first attributed to the pyrolysis of lignin and hemicelluloses, and the second to the presence of resin, tannin, pigments, etc. [35]. Similarly, the main decomposition of pinecones in an inert atmosphere (nitrogen) occurs in the temperature range of 200–500 °C [8]. Another study analyzed the pyrolysis of biomass, showing that the weight loss of hemicelluloses occurred at 220–315 °C and cellulose at 315–400 °C, while the lignin was more difficult to decompose, encompassing a wide range of temperature between 160 and 900 °C [36].

In conclusion, the morphological and thermal analyses reveal features that reinforce their applicability as biosorbents.

4.3. Adsorption Process

The adsorption of Zn ions onto SPCs demonstrated high efficiency, with removal rates reaching 96%. The influence of particle size on Zn(II) removal efficiency was negligible (Table 3), with removal rates consistently around 96% across the tested size range (0.420–<0.177 mm). This can be attributed to the use of a batch suspension adsorption system, where the adsorbent is uniformly dispersed in the solution, allowing for maximal surface area contact between the adsorbent particles and the Zn ions. In the suspension system, finer particle sizes can be advantageous because they provide a greater surface area and more accessible adsorption sites, leading to faster adsorption kinetics and higher removal efficiency. Moreover, suspension adsorption avoids the issue of flow resistance since there is no fluid passing through a packed structure. In contrast, in fixed-bed column systems, particle size plays a much more critical role, with smaller particles often leading to practical limitations, such as dropping pressure, flow channeling, or even column clogging. These factors make fixed-bed adsorption less suitable for very fine particles, particularly in continuous flow treatment processes. In this study, the batch suspension method was deliberately chosen because it facilitates a more controlled laboratory assessment of adsorption potential, enables efficient contact between adsorbate and adsorbent, and eliminates concerns related to pressure drop and flow obstruction.

Additionally, the observed increase in adsorption efficiency with rising adsorbent concentration—from 1 to 4 g L^{-1} (Figure 5)—further supports the applicability of SPCs in such suspension-based treatment approaches.

Similar results were observed for clarified sludge, rice husk ash, activated alumina, and neem bark: increasing the adsorbent dosage from 2.5 to 30 g L^{-1}, the adsorption of Zn increased, with the maximum removal rate achieved at 10 g L^{-1} [18]. However, for *Sargassum ilicifolium*, the removal rate of Zn, Cu, and Ni ions decreased with increasing the biomass dosage from 0.2 to 1.4 g L^{-1} [23].

Milled pinecone was used as a biosorbent to remove Cd, Pb, Cu, and Cr(VI) from aqueous solution [11]. An amount of 2 g L^{-1} was the optimum dosage, at pH 5.5, to remove Cu and Pb, while for Cd, the dose of 5 g L^{-1}, at the same pH, showed the best result. For Cr(VI), the best adsorption rate was achieved with 10 g L^{-1}, at pH 2.

The pH plays a significant role in the adsorption process. SPCs exhibited high Zn(II) removal efficiency (93–98%) across the pH range of 3–9 (Figure 6), with a slight upward trend at higher pH values. However, the potential precipitation of $Zn(OH)_2$ above pH 8 required the selection of pH 7 as the optimal operating condition to ensure adsorption predominance over precipitation. This is in accordance with the pHpzc value of 5.2. When the pH of the solution is under the pHpzc, the surface is positively charged, which causes electrostatic repulsion between ions and the biosorbent surface, while, on the contrary, when the pH of the solution is above the pHpzc, the surface becomes negatively charged, heading to electrostatic attraction [37]. A few results have been reported for other biosorbents, e.g., the ideal pH for the removal of zinc onto clarified sludge, rice husk ash, neem bark, and activated alumina was pH 5.0 [18], and pH 6.0 for *Lemna gibba* [21] and a hydroxyapatite–biochar nanocomposite [37].

A clear decreasing trend in the adsorption rate was observed as the initial metal ion concentration increased from 10 to 50 mg L^{-1}, with the adsorption rate decreasing from approximately 98.8% to 95.4% (Figure 7). This suggests that stone pinecones possess a high affinity for Zn^{2+} ions, which is particularly highlighted at lower concentrations. At lower initial concentrations (10–20 mg L^{-1}), the number of Zn^{2+} ions in solution is relatively low compared to the available active sites on the surface of the adsorbent. This leads to nearly complete utilization of the ions by the abundant functional groups (e.g., hydroxyl, carboxyl) present in the lignocellulosic structure of the stone pinecones, therefore resulting in a very

high removal efficiency. However, as the initial concentration increases, the number of Zn^{2+} ions begins to exceed the available adsorption sites, and a gradual, although moderate, decline in removal efficiency occurs due to site saturation and increased competition among metal ions for limited binding sites. The high adsorption efficiency observed, even at the higher metal concentrations, highlights the potential of stone pinecones as a low-cost and effective biosorbent for Zn^{2+} ion removal from aqueous solutions. It is also worth noting that the relatively small standard error bars indicate good reproducibility and reliability of the experimental data. This means that the trituration and mixing of pinecones allows an adsorbent homogeneity that overcomes the natural variability of individual pinecones.

The adsorption process follows the Freundlich model (R^2 = 0.99, Table 4), which designates that the retention of ions occurs in a multilayer form in the SPC surface, indicating a heterogeneous energy distribution of active sites. This is in accordance with the surface heterogeneity observed in the SEM images (Figure 2). On the contrary, the removal of Pb by pinecone-activated carbon follows the Langmuir model (R^2 = 0.99) [31]. Similarly, the removal of Cu and Cr(VI) by pinecones fitted the Langmuir model, while the best model to describe the adsorption of Pb and Cd was the Langmuir–Freundlich isotherm [11].

The maximum adsorptive capacity of SPCs for Zn ions was found to be 7.92 mg g^{-1}, similar to the adsorption of Pb by pinecones of 6.78 mg g^{-1} [1]. A very similar adsorptive capacity of 7.90 mg g^{-1} of Zn ions was reported when using *Ziziphus joazeiro* barks [22]. Activated carbons have higher adsorption capacity, as described for pinecone (*Pinus nigra*)-activated carbon, which showed a maximum adsorption capacity of Pb of 27.53 mg g^{-1} [31]. Since SPCs show a predominantly crystalline cellulose structure, the maximum adsorption capacity may have been limited by this factor.

Figure 9 illustrates the effect of contact time on the adsorption efficiency of Zn^{2+} ions onto stone pinecones, with measurements taken from 15 min up to 360 min. The adsorption rate remains consistently high, fluctuating slightly around 97.5–98.1%, indicating that equilibrium is reached rapidly and maintained over an extended period. The high initial adsorption rate suggests that most of the available binding sites on the stone pinecone surface are readily accessible and that Zn^{2+} ions are rapidly adsorbed due to a strong affinity between the metal ions and the functional groups on the biosorbent. The minor variations observed over time likely reflect experimental variability rather than a significant change in adsorption behavior. Importantly, the lack of a significant increase in adsorption with time beyond the first 15 min implies that equilibrium is reached quickly, making the process highly efficient for practical applications. In fact, rapid equilibrium is advantageous in large-scale water treatment processes, as it reduces the required contact time and thus operational costs.

The kinetics experiments (Figure 8, Table 5) showed that the adsorption is mostly chemisorption, following the PSO model (R^2 = 1). This kinetic model states that chemical bonds occur between adsorbate and adsorbent functional groups located on the surface, which is confirmed by the low surface area determined by BET, indicating that the amount of mesopores and micropores was very low. Similarly, the adsorption of Pb [10], Cu, and Cd [14] onto pinecones also followed the pseudo-second-order kinetic model, with R^2 between 0.99 and 1.

Nevertheless, the other models tested (PFO, Elovich, and ID) also showed good correlation with the experimental data, which indicates that more than one mechanism may take place during the process.

5. Conclusions

Stone pinecones (SPCs) exhibit physicochemical and structural properties suitable for application as biosorbents. Their chemical composition—comprising a diverse array of

functional groups derived from extractives, lignin, and polysaccharides—combined with a heterogeneous, porous morphology and extensive surface area, facilitates efficient sorption. In aqueous systems, SPCs achieved Zn(II) removal efficiencies of approximately 96% at pH 7, with a maximum adsorption capacity of 7.92 mg g^{-1}. The equilibrium data were best described by the Freundlich isotherm model, indicating a heterogeneous adsorption surface and multilayer uptake, while kinetic analysis followed a pseudo-second-order model, consistent with chemisorption as the predominant mechanism.

Therefore, *Pinus pinea* cones are a promising, eco-friendly, and cost-effective biosorbent for the removal of heavy metals from aqueous solutions, with clear potential for integration into water treatment technologies. Future work will focus on the application of this biosorption process to real industrial wastewater and on assessing the effects of pre-treatment or activation strategies on adsorption efficiency. Such studies may enable optimization under practical waste management conditions and expand the operational scope of SPC-based treatment systems.

Author Contributions: Conceptualization, M.M. and H.P.; methodology, M.M., H.P., L.C.-L., B.E., and I.S.-V.; software, M.M., I.S.-V., and L.C.-L.; investigation, M.M.; writing—original draft preparation, M.M.; writing—review and editing, M.M., H.P., L.C.-L., B.E., L.G., and I.S.-V.; supervision, H.P., L.C.-L., B.E., and L.G. All authors have read and agreed to the published version of the manuscript.

Funding: This research was funded by national funds through the FCT—Foundation for Science and Technology, I.P., by a doctoral scholarship with the reference number 2023.03677.BDANA (DOI 10.54499/2023.03677.BDANA); by the CERNAS-IPV Research Centre under the project UIDB/00681, (DOI 10.54499/UIDP/00681/2020); and by the Forest Research Centre (CEF), within the scope of the projects UIDB/00239/2020 (DOI 10.54499/UIDB/00239/2020).

Data Availability Statement: The original contributions presented in this study are included in the article. Further inquiries can be directed to the corresponding authors.

Acknowledgments: The authors would like to thank the Polytechnic Institute of Viseu and the University of Aveiro for their support.

Conflicts of Interest: Author Lucas Grosche was employed by the company 4iTec Lusitânia S.A., Lugar do Pombal, Zona Industrial do Salgueiro. The remaining authors declare that the research was conducted in the absence of any commercial or financial relationships that could be construed as a potential conflict of interest.

References

1. Martín-Lara, M.A.; Blázquez, G.; Calero, M.; Almendros, A.I.; Ronda, A. Binary Biosorption of Copper and Lead onto Pine Cone Shell in Batch Reactors and in Fixed Bed Columns. *Int. J. Miner. Process.* **2016**, *148*, 72–82. [CrossRef]
2. Shaikhiev, I.G.; Kraysman, N.V.; Sverguzova, S.V. World Experience in Using Pine Cones to Remove Various Pollutants from Aquatic Environments. *Mater. Int.* **2025**, *7*, 29.
3. Nergiz, C.; Dönmez, İ. Chemical Composition and Nutritive Value of *Pinus pinea* L. Seeds. *Food Chem.* **2004**, *86*, 365–368. [CrossRef]
4. Sousa, J.L.C.; Ramos, P.A.B.; Freire, C.S.R.; Silva, A.M.S.; Silvestre, A.J.D. Chemical Composition of Lipophilic Bark Extracts from *Pinus pinaster* and *Pinus pinea* Cultivated in Portugal. *Appl. Sci.* **2018**, *8*, 2575. [CrossRef]
5. Calama, R.; Gordo, J.; Mutke, S.; Conde, M.; Madrigal, G.; Garriga, E.; Arias, M.J.; Piqué, M.; Gandía, R.; Montero, G.; et al. Decline in Commercial Pine Nut and Kernel Yield in Mediterranean Stone Pine (*Pinus pinea* L.) in Spain. *Iforest—Biogeosciences For.* **2020**, *13*, 251. [CrossRef]
6. Ayrilmis, N.; Buyuksari, U.; Avci, E.; Koc, E. Utilization of Pine (*Pinus pinea* L.) Cone in Manufacture of Wood Based Composite. *For. Ecol. Manag.* **2009**, *259*, 65–70. [CrossRef]
7. ICNF. *Perfil Florestal—Portugal*; Instituto da Conservação da Natureza e das Florestas: Lisbon, Portugal, 2021; p. 4.
8. Almendros, A.I.; Martín-Lara, M.A.; Ronda, A.; Pérez, A.; Blázquez, G.; Calero, M. Physico-Chemical Characterization of Pine Cone Shell and Its Use as Biosorbent and Fuel. *Bioresour. Technol.* **2015**, *196*, 406–412. [CrossRef]

9. Ben Amar, M.; Mallek, M.; Valverde, A.; Monclús, H.; Myers, T.G.; Salvadó, V.; Cabrera-Codony, A. Competitive Heavy Metal Adsorption on Pinecone Shells: Mathematical Modelling of Fixed-Bed Column and Surface Interaction Insights. *Sci. Total Environ.* **2024**, *917*, 170398. [CrossRef] [PubMed]
10. Bagherian, G.; Nemati, E.; Arab Chamjangali, M.; Ashrafi, M. Removal of Lead Ions from Aqueous Solutions Using Functionalized Pine Cone Powder. *J. Iran. Chem. Soc.* **2021**, *18*, 2369–2379. [CrossRef]
11. Amar, M.B.; Walha, K.; Salvadó, V.; Salvestrini, S. Valorisation of Pine Cone as an Efficient Biosorbent for the Removal of Pb(II), Cd(II), Cu(II), and Cr(VI). *Adsorpt. Sci. Technol.* **2021**, *2021*, 6678530. [CrossRef]
12. Şen, A.; Pereira, H.; Olivella, M.A.; Villaescusa, I. Heavy Metals Removal in Aqueous Environments Using Bark as a Biosorbent. *Int. J. Environ. Sci. Technol.* **2015**, *12*, 391–404. [CrossRef]
13. Sharma, A.K.; Ghodke, P.K.; Goyal, N.; Bobde, P.; Kwon, E.E.; Lin, K.-Y.A.; Chen, W.-H. A Critical Review on Biochar Production from Pine Wastes, Upgradation Techniques, Environmental Sustainability, and Challenges. *Bioresour. Technol.* **2023**, *387*, 129632. [CrossRef]
14. Değirmen, G.; Kılıç, M.; Çepelioğullar, Ö.; Pütün, A.E. Removal of Copper(II) and Cadmium(II) Ions from Aqueous Solutions by Biosorption onto Pine Cone. *Water Sci. Technol.* **2012**, *66*, 564–572. [CrossRef]
15. Gundogdu, A.; Ozdes, D.; Duran, C.; Bulut, V.N.; Soylak, M.; Senturk, H.B. Biosorption of Pb(II) Ions from Aqueous Solution by Pine Bark (*Pinus brutia* Ten.). *Chem. Eng. J.* **2009**, *153*, 62–69. [CrossRef]
16. González-Feijoo, R.; Santás-Miguel, V.; Arenas-Lago, D.; Álvarez-Rodríguez, E.; Núñez-Delgado, A.; Arias-Estévez, M.; Pérez-Rodríguez, P. Effectiveness of Cork and Pine Bark Powders as Biosorbents for Potentially Toxic Elements Present in Aqueous Solution. *Environ. Res.* **2024**, *250*, 118455. [CrossRef]
17. Taty-Costodes, V.C.; Fauduet, H.; Porte, C.; Delacroix, A. Removal of Cd(II) and Pb(II) Ions, from Aqueous Solutions, by Adsorption onto Sawdust of *Pinus sylvestris*. *J. Hazard. Mater.* **2003**, *105*, 121–142. [CrossRef]
18. Bhattacharya, A.K.; Mandal, S.N.; Das, S.K. Adsorption of Zn(II) from Aqueous Solution by Using Different Adsorbents. *Chem. Eng. J.* **2006**, *123*, 43–51. [CrossRef]
19. Cutillas-Barreiro, L.; Paradelo, R.; Igrexas-Soto, A.; Núñez-Delgado, A.; Fernández-Sanjurjo, M.J.; Álvarez-Rodriguez, E.; Garrote, G.; Nóvoa-Muñoz, J.C.; Arias-Estévez, M. Valorization of Biosorbent Obtained from a Forestry Waste: Competitive Adsorption, Desorption and Transport of Cd, Cu, Ni, Pb and Zn. *Ecotoxicol. Environ. Saf.* **2016**, *131*, 118–126. [CrossRef]
20. Morales-Barrera, L.; Cristiani-Urbina, E. Equilibrium Biosorption of Zn^{2+} and Ni^{2+} Ions from Monometallic and Bimetallic Solutions by Crab Shell Biomass. *Processes* **2022**, *10*, 886. [CrossRef]
21. Morales-Barrera, L.; Flores-Ortiz, C.M.; Cristiani-Urbina, E. Single and Binary Equilibrium Studies for Ni^{2+} and Zn^{2+} Biosorption onto Lemna Gibba from Aqueous Solutions. *Processes* **2020**, *8*, 1089. [CrossRef]
22. Santos, Y.T.d.C.; da Costa, G.P.; Menezes, J.M.C.; Nunes, J.V.S.; Hosseini-Bandegharaei, A.; Coutinho, H.D.M.; Júnior, D.S.; Filho, F.J.d.P.; Teixeira, R.N.P. Adsorption of Zn(II) IONS by *Ziziphus joazeiro* Barks in Aqueous Solutions. *Results Chem.* **2024**, *7*, 101339. [CrossRef]
23. Tabaraki, R.; Nateghi, A. Multimetal Biosorption Modeling of Zn^{2+}, Cu^{2+} and Ni^{2+} by *Sargassum ilicifolium*. *Ecol. Eng.* **2014**, *71*, 197–205. [CrossRef]
24. *T 204 cm-17*; Solvent Extractives of Wood and Pulp, Test Method. Technical Association of the Pulp & Paper Industry (TAPPI): Peachtree Corners, GA, USA, 2017.
25. *T 203*; Alpha-, beta- and gamma-cellulose in pulp. Technical Association of the Pulp & Paper Industry (TAPPI): Peachtree Corners, GA, USA, 2008.
26. *T 222 om-21*; Acid Insoluble Lignin in Wood and Pulp. Technical Association of the Pulp & Paper Industry (TAPPI): Peachtree Corners, GA, USA, 2002.
27. Bangaraiah, P.; Sarath Babu, B.; Abraham Peele, K.; Rajeswara Reddy, E.; Venkateswarulu, T.C. Removal of Multiple Metals Using Tamarindus Indica as Biosorbent through Optimization of Process Variables: A Statistical Approach. *Int. J. Environ. Sci. Technol.* **2020**, *17*, 1835–1846. [CrossRef]
28. Gonultas, O.; Ucar, M.B. Characteristics of Pinus. *Lignocellulose* **2013**, *2*, 262–269.
29. Santos, J.; Pereira, J.; Ferreira, N.; Paiva, N.; Ferra, J.; Magalhães, F.D.; Martins, J.M.; Dulyanska, Y.; Carvalho, L.H. Valorisation of Non-Timber by-Products from Maritime Pine (*Pinus pinaster*, *Ait*) for Particleboard Production. *Ind. Crops Prod.* **2021**, *168*, 113581. [CrossRef]
30. Ucar, M.B.; Ucar, G. Lipophilic Extractives and Main Components of Black Pine Cones. *Chem. Nat. Compd.* **2008**, *44*, 380–383. [CrossRef]
31. Momčilović, M.; Purenović, M.; Bojić, A.; Zarubica, A.; Ranđelović, M. Removal of Lead(II) Ions from Aqueous Solutions by Adsorption onto Pine Cone Activated Carbon. *Desalination* **2011**, *276*, 53–59. [CrossRef]
32. Ouafi, R.; Omor, A.; Gaga, Y.; Akhazzane, M.; Taleb, M.; Rais, Z. Pine Cones Powder for the Adsorptive Removal of Copper Ions from Water. *Chem. Ind. Chem. Eng. Q.* **2021**, *27*, 341–354. [CrossRef]
33. Sahin, H.T.; Yalcin, O.U. Conifer Cones: An Alternative Raw Material for Industry. *J. Pharm. Res. Int.* **2017**, *17*, 1–9. [CrossRef]

34. Almendros, A.I.; Calero, M.; Ronda, A.; Martín-Lara, M.A.; Blázquez, G. Influence of Nickel during the Thermal Degradation of Pine Cone Shell. Study of the Environmental Implications. *J. Clean. Prod.* **2018**, *183*, 403–414. [CrossRef]
35. Chen, Y.; Wang, L.; Zhao, M.; Ma, H.; Chen, D.; Zhang, Y.; Zhou, J. Comparative Study on the Pyrolysis Behaviors of Pine Cone and Pretreated Pine Cone by Using TGA–FTIR and Pyrolysis-GC/MS. *ACS Omega* **2021**, *6*, 3490–3498. [CrossRef]
36. Yang, H.; Yan, R.; Chen, H.; Lee, D.H.; Zheng, C. Characteristics of Hemicellulose, Cellulose and Lignin Pyrolysis. *Fuel* **2007**, *86*, 1781–1788. [CrossRef]
37. Wang, Y.-Y.; Liu, Y.-X.; Lu, H.-H.; Yang, R.-Q.; Yang, S.-M. Competitive Adsorption of Pb(II), Cu(II), and Zn(II) Ions onto Hydroxyapatite-Biochar Nanocomposite in Aqueous Solutions. *J. Solid State Chem.* **2018**, *261*, 53–61. [CrossRef]